Observation of a Discrete Family of Dissipative Solitons in a Nonlinear Optical System

M. Pesch, E. Große Westhoff, T. Ackemann,* and W. Lange

Institut für Angewandte Physik, Westfälische Wilhelms–Universität Münster, Corrensstrasse 2/4, D-48149 Münster, Federal Republic of Germany

(Received 27 March 2005; published 30 September 2005)

We report on the observation of a discrete family of spatial dissipative solitons in a simple optical pattern forming system, which is based on a modified single-mirror feedback arrangement. After a pitchfork bifurcation the system possesses two (nearly) equivalent coexisting states of different polarizations. The spatial solitons correspond to excursions from one of the two states serving as a background state towards the other one. The members of the soliton family differ in the number of high-amplitude radial oscillations. The observations are in good agreement with numerical simulations and general expectations for dissipative solitons.

DOI: 10.1103/PhysRevLett.95.143906 PACS numbers: 42.65.Tg, 05.45.Yv, 42.65.Sf

Solitonlike localized states in dissipative systems driven far from thermal equilibrium found considerable interest in a vast variety of systems, e.g., hydrodynamics [1], granular media [2], gas discharges [3], and nonlinear optics [4–11]. Often these structures are referred to as ''dissipative solitons'' or ''autosolitons.'' One of the intriguing features of these structures is that they are attractors of the dynamics, i.e., width and amplitude are fixed by the parameters and independent of the initial conditions. This is in strong contrast to the conservative case where a soliton is part of a one-parameter family of varying width and amplitude [12]. However, several theoretical studies on different model systems show that the spatial dissipative soliton is not necessarily unique, but that a sequence of higher-order solitons might exist (and be stable) that differ in their internal structure (e.g., the number of radial oscillations) [13–18]. To the best of our knowledge, there are no corresponding experimental observations.

We report on the observation of a discrete family of solitons in a nonlinear optical system displaying a symmetry-breaking bifurcation to two equivalent (or nearly equivalent) states. This frequently encountered situation had been shown before to support the existence of solitons in nonlinear optical systems, e.g., in theoretical models of optical parametric oscillators [18–20], cavities filled with a vectorial generalization of a Kerr medium [21], intracavity second harmonic generation [17], and intracavity four-wave mixing [22]. In the latter case the (fundamental) soliton was also observed experimentally [22].

The system under study here is an implementation of the well-known single-mirror feedback arrangement [23] (see Fig. 1). The driving light field is a linearly polarized collimated laser beam ($w_0 = 1.89$ mm), which is spatially filtered in order to get a good cylindrical symmetry. This ''holding beam'' is injected into a heated cell containing sodium vapor in a nitrogen buffer gas atmosphere as the nonlinear medium. The laser is operated at a frequency some linewidths above the sodium D_1 line.

The feedback loop consists of the feedback mirror ($R = 0.99$) at a distance d behind the medium and a $\lambda/8$-retardation plate, which represents a modification with respect to the standard scheme [24]. Because of its presence, the reentrant field will be elliptically polarized unless the polarization vector of the impinging field is exactly parallel to one of the principal axes of the $\lambda/8$ plate. The portion of light that is transmitted by the feedback mirror is used for detection. The exit plane of the sodium cell is imaged onto a CCD camera. A second $\lambda/8$ plate whose optical axes are oriented perpendicular to the ones of the first reestablishes the polarization state of the light field in front of the first $\lambda/8$ plate before detection. A linear polarizer (''analyzer'') is used for analyzing the polarization state of the light field. In addition to the wide holding beam, there is a focused beam that can be switched on and off. Its polarization and spot size in the cell can be adjusted. Its frequency is slightly shifted with respect to the one of the holding beam to avoid interference effects. We call this beam ''addressing beam.''

Optical pumping with circularly polarized light induces a nonzero ''orientation'' of the vapor whose sign depends on the helicity of the light. Under the conditions of the experiment, the sodium D_1 line can be modeled as a $J = 1/2 \rightarrow J' = 1/2$ transition with the population of the excited state being negligible (see [25] and references therein). Under this assumption, the orientation is simply

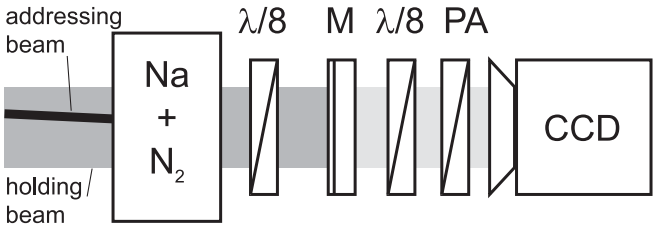

FIG. 1. Schematic experimental setup. $\lambda/8$: eighth-wave plate; M: mirror; PA: polarization analyzer; CCD: charge-coupled device camera.

given by the normalized population difference between the two Zeeman sublevels of the ground state (ranging from -1 to $+1$). For a linearly polarized input no net pumping should occur if the slow axis of the $\lambda/8$ plate is aligned with the axis of the input polarization. However, it is known that this system shows spontaneous symmetry breaking between two spatially homogeneous elliptically polarized states of opposite helicity [24,26]. One state is connected with a positive orientation of the medium and a positive rotation of the main axis of polarization, and the other one has a negative orientation and polarization rotation. This symmetry breaking can be interpreted as a pitchfork bifurcation. If the slow axis of the $\lambda/8$ plate is slightly rotated by an angle Φ with respect to the input polarization, a perturbed pitchfork bifurcation is observed. At much higher pump levels both of these homogeneous branches become unstable against a modulational instability, and pattern formation and the existence of a polarization domain wall were demonstrated [24].

In this parameter region, the ignition of a solitary structure was found to be possible (see Fig. 2). The system is prepared in the state with negative polarization rotation. The analyzer is adjusted such that this ''background beam'' is suppressed [Fig. 2(a)]. Then the σ_+-polarized addressing beam is switched on and induces locally a transition to a state with positive polarization rotation. This results in a high transmission through the analyzer [Fig. 2(b)]. If the addressing beam is switched off, a stable solitary structure survives that consists of a bright ring [Fig. 2(c)]. Switching on—at the position of the solitary structure—the addressing beam with σ_- polarization results in an extinction of the solitary structure [Fig. 2(d)]. After the erasure procedure, the system recovers its initial state [Fig. 2(e)]. A similar structure can be ignited by means of a σ_--polarized beam, if the system is first brought into a state with positive polarization rotation.

If the diameter of the addressing beam is enlarged, other types of stable solitary structures can be ignited for the same or similar parameters (see below). The solitons differ in size and in the number of radial oscillations (see Fig. 3).

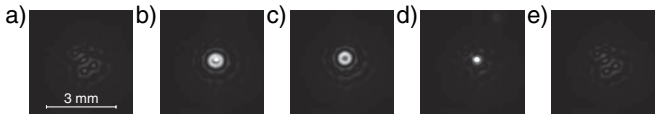

FIG. 2. Switching sequence of a solitary structure. Polarization analyzer aligned for suppression of the background beam in the detection branch: (a) background beam; (b) ignition of a soliton with circularly polarized addressing beam; (c) stable soliton with addressing beam switched off; (d) erasure of soliton with addressing beam of opposite circular polarization; (e) background beam. Parameters: mirror distance $d = 120$ mm; buffer gas pressure $p_{N_2} = 300$ mbar; cell temperature $T = 321.8\,^{\circ}$C; laser detuning $\Delta = 16.2$ GHz; laser power $P_{\mathrm{las}} = 219$ mW; rotation of the slow axis of the eighth-wave plate with respect to input polarization $\Phi = 4^{\circ}30'$.

We denote their order by numbering them from 1–4. Depending on the size of the addressing beam, the circular domain, which is initially ignited, will shrink or expand until one of the stable solitary structures is reached. The spatial frequency of the radial oscillations corresponds quite accurately to the length scale of the modulational instability. Soliton 4 is very sensitive to the experimental parameters. We mention that it is slightly off-center, though it was ignited at beam center. Not all orders of solitons depicted in Fig. 3 are observed for the same set of parameters, though the regions of existence of solitons of subsequent orders typically overlap.

The existence of a discrete family of solitons can be reproduced in numerical simulations of the microscopic model described in Ref. [25]; the inclusion of the action of the $\lambda/8$ plate is readily accomplished (see Ref. [24]). For parameter values similar to those used in the experiment, the four observed types of solitons differing by the number of radial oscillations are found [see Figs. 4(b)–4(e)]. The results match nicely the experimental observations (cf. Fig. 3). Just as in the experiment large structures that are ignited in the beam center drift to an off-center position. The drift is attributed to the amplitude and phase gradients originating from the inhomogeneous pumping by the Gaussian beam [27]; see also [6,13,28] for drift phenomena due to gradients.

In the numerical simulations, soliton 4 was found to be only ''metastable'' for a beam radius of $w_0 = 1.89$ mm; i.e., it drifts very slowly to the boundary and then either decays into soliton 3 or expands and switches the whole beam to the slightly patterned state with positive polarization rotation. For a slightly larger beam radius [$w_0 = 2.2$ mm, Figs. 4(e) and 4(k)] it is stable. This provides further support for the assumption that high-order solitons are disfavored in a Gaussian beam. This is probably due to the rather large size of the structures (diameters range from 0.41 mm for soliton 1 to 1.58 mm for soliton 4) in comparison to the beam radius ($w_0 \approx 1.9$ mm).

In contrast to the experiment, the numerical simulations also give the orientation of the sodium vapor. It is shown in Figs. 4(g)–4(l). It can be seen that the number of radial oscillations of the solitons is reduced by one with respect to the intensities in Figs. 4(b)–4(e); i.e., soliton 1 is single humped and can be identified as the fundamental soliton.

The solitons can also be found in simulations with plane wave input. The orientation distributions are shown in

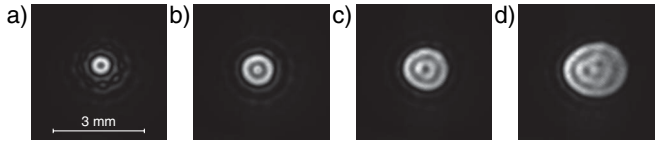

FIG. 3. Experimentally observed solitons. Parameters as in Fig. 2 with the exception of the replacements $T = 327.3\,^{\circ}$C, $\Delta = 14.6$ GHz, $P_{\mathrm{las}} = 165$ mW, $\Phi = 7^{\circ}00'$ in (b) to (d).

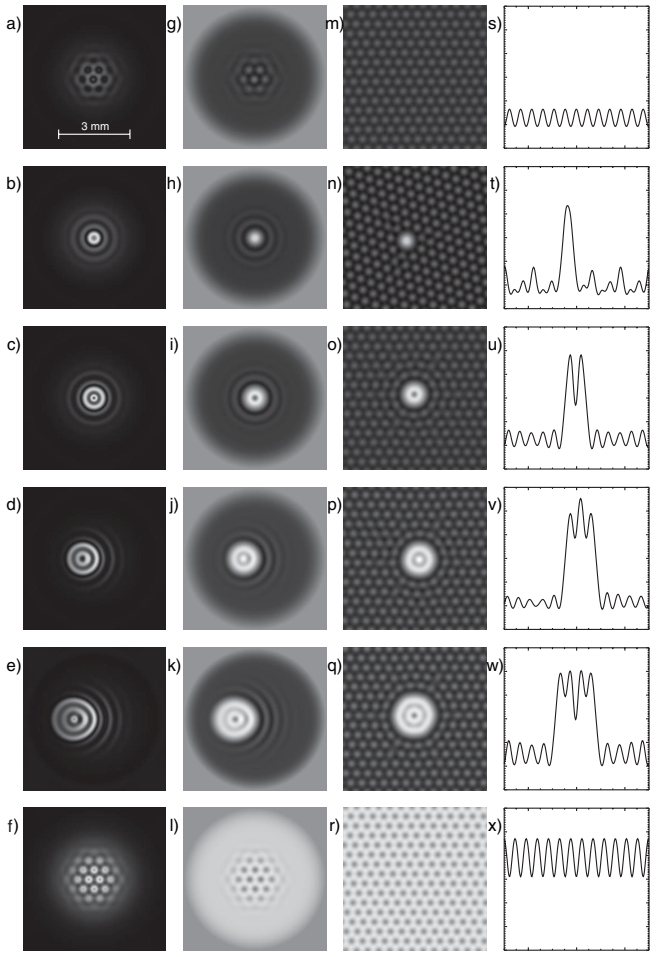

FIG. 4. Numerically obtained structures. First column: Transmitted intensity in the field component orthogonal to the polarization of the background beam. Second column: Orientation distributions corresponding to first column. Orientation set to zero at a radius of 3 mm to simulate depolarization of the vapor at the cell walls in simulations with Gaussian beam input. Third column: Orientation distributions in simulations with plane wave input. Fourth column: Horizontal cuts through orientation distribution; ordinate scale extends from -0.3 to 0.3. First row: Slightly patterned state with negative orientation. Second to fifth rows: Solitons of different orders. Sixth row: Slightly patterned state with positive orientation. Parameters: $d = 120$ mm, ground state relaxation rate $\gamma = 200\ \mathrm{s}^{-1}$, relaxation rate of optical coherences $\Gamma_2 = 9.94 \times 10^9\ \mathrm{s}^{-1}$, $\Delta = 11.9$ GHz, diffusion constant $D = 255\ \mathrm{mm}^2\,\mathrm{s}^{-1}$, particle density $N = 4.65 \times 10^{19}\ \mathrm{m}^{-3}$, length of heated zone $L = 15$ mm, mirror reflectivity $R = 99.5\%$. (a)–(l) pump rate in beam center $P_0 = 180 \times 10^3\ \mathrm{s}^{-1}$, beam radius $w_0 = 1.89$ mm except (e),(k) $w_0 = 2.2$ mm, (m)–(x) $P_0 = 130 \times 10^3\ \mathrm{s}^{-1}$ except (n),(t) $P_0 = 150 \times 10^3\ \mathrm{s}^{-1}$; (a),(g),(c),(i),(f),(l) $\Phi = 15°30'$; (b),(h) $\Phi = 19°30'$; (d),(j),(e),(k) $\Phi = 9°30'$; (m),(s),(o),(u),(r),(x) $\Phi = 13°00'$; (n),(t) $\Phi = 21°00'$; (p),(v) $\Phi = 8°00'$; (q),(w) $\Phi = 5°00'$.

Figs. 4(m)–4(r), and horizontal cuts through the center are displayed in Figs. 4(s)–4(x). The first and sixth rows of Fig. 4 show the manifestations of the two coexisting branches emerging from the pitchfork bifurcation, which are represented by either a positive [Figs. 4(r) and 4(x)] or a negative [Figs. 4(m) and 4(s)] orientation of the medium. On both branches a modulational instability is found in the parameter region where the solitons exist. This results in small-amplitude patterns with hexagonal symmetry [see Figs. 4(m) and 4(r)]. Small-amplitude hexagonal patterns are also found in the experiment (cf. also [24]).

Obviously, the amplitude as well as the width of a constituent of the hexagonal pattern [Fig. 4(s)] and of the fundamental soliton [Fig. 4(t)] are considerably different; i.e., the soliton cannot be interpreted as a single constituent of these hexagonal patterns. Instead, it appears that they represent a localized excursion from the "background state" into the vicinity of the amplitude level of the other state and back; i.e., the soliton represents a homoclinic connection of the background state with itself (see, e.g., [29]). In the one-dimensional case this situation is characterized by the existence of two switching fronts that are locked, while in the two-dimensional case a circular front is interacting with itself. In the interpretation of our experiment we assume that the locking process is heavily supported by the presence of a modulational instability which exists on both branches, i.e., in the states of positive or negative rotation of the polarization. Locking should then be possible at different spatial separations of the fronts due to the periodicity of the modulated states. The existence of a discrete family of solitons appears to be the natural consequence. The assumption of the crucial role of the modulational instability in our experiment is basically supported by the fact that we always observe the wave number of the modulational instability in the Fourier spectrum, if the threshold of soliton formation is surpassed. Far above threshold the solitons even lose their radial symmetry. Some indication of this process can be seen in the experimental [Figs. 3(c) and 3(d)] and numerical results [Fig. 4(q)] presented here.

Our observation of a discrete family of dissipative solitons fits nicely with results obtained in models of nonlinear cavities and in unspecific model equations, where oscillatory tails of the fronts—often, but not always, connected to a modulational instability—were shown to give rise to the existence of a set of solitons differing in size and/or the number of radial oscillations [13,15,16,18]. It should be noted that this general mechanism does not seem to apply to the bistability between two types of solitons (circular and triangular) reported recently [11], which was attributed to the coexistence of a stable homogeneous state and two different pattern forming branches.

A clue to the mechanism stabilizing the solitons is obtained from the following experimental observations. The minimum threshold power P_c for the existence of solitons occurs if the slow axis of the $\lambda/8$ plate and the input polarization include some finite angle Φ_c that dis-

favors the polarization state of the background and favors the polarization state of the soliton. (About the same threshold is obtained for the angle $-\Phi_c$, of course, with the roles of the two polarization states being interchanged.) When the input power is increased above P_c, then there is a finite range of angles Φ, where solitons exist. Above a second threshold P_c' (P_c' about $1.3P_c$ for the parameters considered here) the range of Φ, where solitons exist, includes $\Phi = 0$. In that case the two polarization states are completely equivalent. It is a well-known phenomenon in nonlinear model systems that a circular droplet of one of two equivalent states within the background of the other one shrinks and finally disappears (''curvature-driven dynamics''—see, e.g., [30,31]). The edge of the droplet, however, may be pinned by spatial modulations, and pinning is more probable, when strong modulations are present, of course. Obviously robust pinning occurs in our system when the input power P exceeds P_c'.

If the two homogeneous states are not completely equivalent, i.e., in the case $\Phi \neq 0$, the curvature-driven shrinkage of a droplet is counteracted, if the droplet is in the preferred state. For large values of $|\Phi|$ the shrinkage can even be overcompensated and then the droplet expands. For a given Φ, there is a critical radius of the droplet where the two effects are in balance. However, this situation is known to be unstable in general, at least if the droplet state and the background state are homogeneous [30]. These expectations are confirmed by numerical simulations of our system below the critical value P_c. Because of the existence of the modulational instability, however, spatial modulations become much more pronounced for increased input power. In the case $\Phi = \Phi_c$ the modulations occurring for $P = P_c$ are considered to warrant stabilization, while in the case $\Phi = 0$, i.e., without other effects counteracting the curvature-driven dynamics, the modulations corresponding to P_c' are necessary.

The symmetry-breaking pitchfork bifurcation that underlies the existence of spatial solitons in the system under study is a very common phenomenon in nonlinear physics. It can be expected that the existence of a discrete family of spatial dissipative solitons reported here is also widespread. In our case, however, the occurrence of the solitons is closely linked to the presence of a modulational instability. Though a modulational instability is not a prerequisite for the existence of higher-order solitons in general, it seems to play its role here in their stabilization and may make them more robust and thus facilitate their observation.

We are grateful to P. Coullet and D. Gomila for fruitful discussions and to J. U. Schurek for help in analyzing the experimental data.

*Present address: Department of Physics, University of Strathclyde, Glasgow G4 ONG, U.K.

[1] O. Lioubashevski, H. Arbell, and J. Fineberg, Phys. Rev. Lett. **76**, 3959 (1996).
[2] P. B. Umbanhowar, F. Melo, and H. L. Swinney, Nature (London) **382**, 793 (1996).
[3] C. P. Schenk, P. Schütz, M. Bode, and H.-G. Purwins, Phys. Rev. E **57**, 6480 (1998).
[4] N. N. Rosanov and G. V. Khodova, J. Opt. Soc. Am. B **7**, 1057 (1990).
[5] M. Tlidi, P. Mandel, and R. Lefever, Phys. Rev. Lett. **73**, 640 (1994).
[6] W. J. Firth and A. J. Scroggie, Phys. Rev. Lett. **76**, 1623 (1996).
[7] B. Schäpers, M. Feldmann, T. Ackemann, and W. Lange, Phys. Rev. Lett. **85**, 748 (2000).
[8] S. Barland *et al.*, Nature (London) **419**, 699 (2002).
[9] L. A. Lugiato, IEEE J. Quantum Electron. **39**, 193 (2003).
[10] P. L. Ramazza, U. Bortolozzo, and L. Pastur, J. Opt. A Pure Appl. Opt. **6**, S266 (2004).
[11] U. Bortolozzo, L. Pastur, P. L. Ramazza, M. Tlidi, and G. Kozyreff, Phys. Rev. Lett. **93**, 253901 (2004).
[12] M. Remoissenet, *Waves Called Solitons: Concepts, Experiments* (Springer, Berlin, Heidelberg, New York, 1994).
[13] N. N. Rosanov, *Spatial Hysteresis and Optical Patterns*, Springer Series in Synergetics (Springer, Berlin, 2002).
[14] G.-L. Oppo, A. J. Scroggie, and W. J. Firth, J. Opt. B **1**, 133 (1999).
[15] G. L. Oppo, A. J. Scroggie, and W. J. Firth, Phys. Rev. E **63**, 066209 (2001).
[16] D. Michaelis, U. Peschel, and F. Lederer, Phys. Rev. A **56**, R3366 (1997).
[17] U. Peschel, D. Michaelis, C. Etrich, and F. Lederer, Phys. Rev. E **58**, R2745 (1998).
[18] K. Staliunas and V. J. Sánchez-Morcillo, Phys. Rev. A **57**, 1454 (1998).
[19] S. Longhi, Phys. Scr. **56**, 611 (1997).
[20] M. Tlidi, P. Mandel, and M. Haelterman, Phys. Rev. E **56**, 6524 (1997).
[21] R. Gallego, M. San Miguel, and R. Toral, Phys. Rev. E **61**, 2241 (2000).
[22] V. B. Taranenko, K. Staliunas, and C. O. Weiss, Phys. Rev. Lett. **81**, 2236 (1998).
[23] G. D'Alessandro and W. J. Firth, Phys. Rev. Lett. **66**, 2597 (1991).
[24] E. Große Westhoff, V. Kneisel, Y. A. Logvin, T. Ackemann, and W. Lange, J. Opt. B **2**, 386 (2000).
[25] A. Aumann, T. Ackemann, E. Große Westhoff, and W. Lange, Phys. Rev. E **66**, 046220 (2002).
[26] T. Yabuzaki, T. Okamoto, M. Kitano, and T. Ogawa, Phys. Rev. A **29**, 1964 (1984).
[27] B. Schäpers, T. Ackemann, and W. Lange, IEEE J. Quantum Electron. **39**, 227 (2003).
[28] A. J. Scroggie, J. Jeffers, G. McCartney, and G.-L. Oppo, Phys. Rev. E **71**, 046602 (2005).
[29] P. Coullet, C. Riera, and C. Tresser, Phys. Rev. Lett. **84**, 3069 (2000).
[30] P. Coullet, Int. J. Bifurcation Chaos Appl. Sci. Eng. **12**, 2445 (2002).
[31] D. Gomila, P. Colet, G. L. Oppo, and M. San Miguel, Phys. Rev. Lett. **87**, 194101 (2001).